Available online at www.elixirpublishers.com (Elixir International Journal)

Mechanical Engineering

Elixir Mech. Engg. 90 (2016) 37714-37721

ISSN: 2229-712X

# A Computational Model for Cutting Forces during End Milling Machining of Metal Matrix Composites

M. Siva Teja and P.Suryanarayana Raju

Department of Mechanical Engineering, MITS, Madnapalle Andhra Pradesh India.

**ARTICLE INFO**

**Article history:**

Received: 23 April 2015;

Received in revised form:

8 January 2016;

Accepted: 14 January 2016;

**Keywords**

End milling,

Cutting forces,

Modelling.

**ABSTRACT**

The cutting forces required for machining of a material are important factors in production design that need to be evaluated carefully for newly developed materials. The cutting forces directly influence the power requirement of the machine tool, tool deflection and tool wear, among other things. In this study a computational model will be developed for prediction of cutting forces in end milling of metal matrix composites. Modeling of cutting forces in milling involves evaluation of chip load, instantaneous shear angle, strain rate and temperature dependent shear stress. The computational model will be validated against experimental data from measurements of cutting forces during end milling of composites under different conditions. The validated model will then be used to conduct a parametric study on the influence of feed rate (*f*), depth of cutting (*a*), cutting speed (*v*), and other cutting parameters on the cutting forces generated during the end milling of composites.



## Introduction

Composite materials are materials are made up of two constituent materials that possess different physical and chemical properties. Through these we can produce new engineering materials with better or improved properties like low weight to strength ratio "[1"]. Prominent among the modern composite materials are the Metal Matrix Composites (MMC) which comprise of a continuous metallic matrix in which reinforcement particles are dispersed. The reinforcement could be fibers, whiskers or smaller particles and their volume fraction could range between a few percent to 40%. These MMCs could be fabricated to generate good combination of physical and chemical properties like creating a desired combination of strength, lightweight, and favorable thermal characteristic of the material "[2]". The MMCs which are used in these applications are prepared by different processes such as powder metallurgy and casting, among others. One of the challenges in using of the Metal Matrix composites as an industrial material is that these materials contain high hardness strengthening particles which results in tool wear and causes difficulties in machining of these materials. Therefore precision and high efficiency machining of these materials is currently a problem. In this regard, many researchers are studying the machining behavior of MMCs and such studies on machining also include investigation of turning of MMCs materials "[3]". Most of the research on machining of MMCs deals with experimental analysis on the effect of various cutting process parameters on different tool materials and their tool life, mainly in continuous operations like turning and there are two similar approaches: predictive model and mechanistic model have also been developed which are used to study the effect of operating parameters on the generated cutting forces "[4]". The main objective of machining is to generate a product of desired shape and dimensions along with other quality requirements such are surface finish. The end milling cutting is an extremely popular process in industry because of its efficient machining and versatility. It also increases the productivity and also achieves good surface finish in the design of machine tools with rigid structure. This process is quite versatile and may be used for rough cut as well as finishing of surfaces with features such as peripheries, slots, pockets and also faces of components. Some of the problems which may arise from this end milling process include cutter breakage and also generation of finished surface which does not satisfy the process stability and product specifications. For this a theoretical model is developed which is based on Oxley's predictive machining theory "[5]" and from this the total forces on each tooth segment at every slice of end

## Modeling

Milling is a widely popular manufacturing process in industries because of its versatility in producing difficult shapes such as curved, flat surfaces with good productivity and quality. In cutting of Metal Matrix Composites (MMCs), and in metal cutting, in general, there are several aspects which are known to affect the total cutting forces that are generated. During the end milling or any other cutting, the process should be free from tool and work piece deflections so that good dimensional accuracy and desired surface finish are attained. For this predictive models are required for calculation of cutting forces. These models will be helpful in

- Optimization of the machining process.
- Designing of a cutting tool.
- Estimation machining power requirement.

## Chip load geometry

In milling process, cutter is rotated while work piece is fed at right angle to the rotation of cutter so the un deformed chip thickness is not constant as the path generated by cutter action is trachoidal. But as feed rate is smaller than cutting speed, it is assumed that trajectory of tool is circular. In general end milling is performed using cutters which are cylindrical in shape and consist of a several sharp flutes or cutting edges around the cylindrical periphery of the cutter. Some end milling cutters have cutting edges at the tip of the cuter as well. Such cutters permit end peripheral cutting as well as end cutting. The flutes or cutting edges are mostly helical in shape. This choice of shape for cutting edges reduces impact between the cutter and

Tele:

E-mail addresses: mallelasivateja65@gmail.com

the work piece during engaging of the cutting edge with the work piece. Figure 1 shows a representative end milling cutter with right-hand helix.

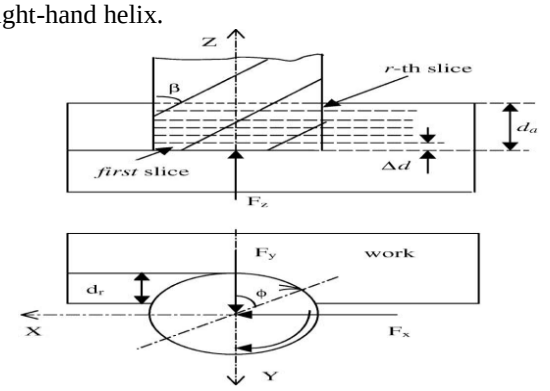


**Fig 1. Representative geometry of a milling cutter** "[6]"

The co-ordinate system used in this study to express the forces has its origin at the point of intersection between the axis of the cutter and the face plane of the cutter. The x-direction is taken to be in the direction opposite to the direction of the feed of the cutter with regard to the work piece. The z-direction is along the axis of the cutter and the normal direction to the feed is taken as the y-direction. Due to the helix angle $h_a$, of milling cutter, the direction of cutting forces changes with the location along the cutter on the axis. In order to model this, the cutter is treated to be made r number of elementary cutters. These elementary cutters are slices made along the axis (i.e. the z-direction) of the whole cutter. The cutting action of each elementary cutter (i.e. each slice cut along the axis) could be modeled using theory of oblique cutting with the inclination angle of each cutting edge of each individual tooth of the elementary cutter approaching the work piece at an angle which will is assumed to be the helix angle ($h_a$). The cutting, thrust and axial forces could thus be computed for each flute of an elementary cutter using oblique cutting theory and components of these forces in global x- y- and z- directions could be found through a directional transformation. The total force on the whole cutter in x- y- and z- directions will be the summation of forces on the elementary cutters.

The time dependent thickness of the un-deformed could be computed using the expression:

$$H_{u,v} = f_t \sin \theta_{u,v}$$

Here $f_t$ denotes the feed per tooth, and $\theta_{u,v}$ is the angular displacement, of the engaged cutting edge of $u^{th}$ tooth in the $v^{th}$ elementary cutter ($v^{th}$ slice), which is measured in clockwise direction with respect to negative y-axis. The index of the cutting flute, u, takes a value between 1 and $N_t$ , where $N_t$ is total number of flutes (or cutting edges) present around the cutter. The order in which the flutes engage in a cutter with right-hand helix is 1, 2, up to Nt. The index u which identifies a particular cutting slice takes a value between 1 and r, where r is the selected number of slices into which the cutter is assumed to be divided along the axis. In the convention adopted here, the first slice is the at the bottom end of the cutter, as shown in Fig. 1. From simple geometrical considerations, $\theta_{u,v}$ can be found out to be:

$$\theta_{u,v}(t) = 2\pi nt-(u-1)\frac{2\pi}{z} - (v-1)\frac{2d_a \tan h_a}{rD}$$

Here n is rotational speed of the tool, D is the diameter of the cutter and t denotes the time.

**3D oblique cutting model**

Here a mathematical model for oblique cutting which is based on predictive theory of machining proposed by Oxley "[5]" is used to compute the cutting of each elementary cutter or axial slice of the end milling cutter. In this Oxley's model the forces generated during cutting are calculated for given conditions of physical properties of the work piece, geometry of the tool geometry and other operating parameters. In this theory, the estimation of cutting forces is through calculation of local stress values along shear plane and the tool-chip interface plane as a function of the shear angle and physical properties of the work piece material, among others. The shear is then estimated using the criteria that the net forces along the shear plain and those along the tool-chip interface are in equilibrium. The direction of the shear plane and that of the tool–chip interface are taken to be along the direction of maximum shear stress and maximum shear strain rate. After the estimation of the shear angle, the thickness of the chip $t_2$ and the components of cutting forces can be calculated using oblique cutting theory and the input data.

The present model for cutting force prediction accounts for oblique cutting of the peripheral cutting flutes and neglects the cutting of the cutting edge at the end of the tool and the effect of the tool nose radius. In the cutting conditions considered here, the forces which are acting along the cutting, feed and radial directions are $P_1$, $P_2$, $P_3$ as shown in figure 2

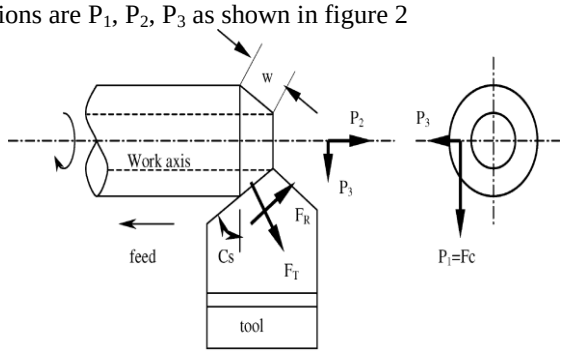


**Fig 2. model for simple oblique cutting** "[6]"

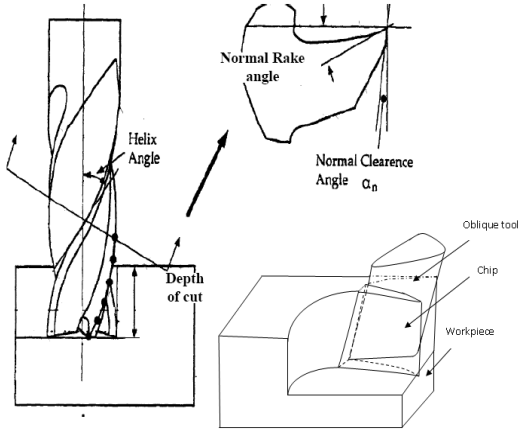


**Fig 3. Geometry of an end mill** "[9]"

Where

$$P_1 = d F_c,$$
$$P_2 = dF_t \cos C_s + dF_t \sin C_s$$
$$P_3 = dF_t \sin C_s - dF_t \cos C_s$$

Here $C_s$ is the side cutting edge angle of the tool and $dF_c$, $dF_t$, $dF_r$ are respectively the components of the cutting force in three mutually perpendicular directions viz., cutting direction, feed direction and radial direction. For the case where $C_s$=0 the force components could be computed using equations

$$dF_c = dr \cos(\beta - \alpha)$$
$$dF_t = dr \sin(\beta - \alpha)$$
$$dF_r = \frac{dF_c(\sin i - \cos i \sin \alpha \tan c_f) - dF_t \cos \alpha \tan c_f}{\sin i \sin \alpha \tan c_f + \cos i}$$

Here $\alpha$ is the rake angle, $\beta$ is friction angle and i is inclination angle, $C_f$ is chip flow angle. Also, dr denotes the net

force along the shear plane as well as the interface between tool and the chip.
Where

$$dr = \frac{N_{AB} t_1 w}{\sin \emptyset \cos(\emptyset+\beta-\alpha)}$$

Here $N_{AB}$ is flow stress, w is width of cut, $t_1$ is the thickness of uncut chip and $\emptyset$ denotes the shear angle.

The shear angle $\emptyset$ is determined using the condition that for the given conditions of tool geometry, material properties etc., the shear intensity along the interface between the tool and chip calculated using the net cutting force dr must be same as the shear flow stress of the work piece material shear (i. e. chip material), which is in turn dependent on the rate at which strain is increasing during cutting and the generated local temperatures in the chip formation under the given conditions. The estimation of the shear angle generally requires iterations to find the value of the angle at which the shear stress at the interface and the shear flow stress of the work piece material become the same. In case there are several shear angles which meet the specified criteria, the largest of those angles is selected such that the minimum work condition is satisfied.

**Evaluation of flow stress**

In machining process, work material experiences large strain, high strain rates and high temperature, which influence its flow stress $N_{AB}$. Therefore, to determine flow stress $N_{AB}$ in machining under high temperature, high strain and strain rate, the model proposed by Johnson and Cook is employed. The Johnson-cook model is mathematically concise and found to be accurate for wide range of materials including aluminium alloys "[7]". In this model, the flow stress is given by:

$$N_{AB} = (A+B.\varepsilon^n)(1+C.\ln \dot{\varepsilon})(1-(\frac{T-T_o}{T_m-T_o})^m$$

In the Johnson-Cook model which is given by the above equation, it is hypothesized that the flow stress of a material will be the product of contributions from the amount of induced strain, the rate of strain and the effects of high temperatures generated which include thermal softening, work hardening, and strain-rate hardening. In the above equation the component *A* indicates the original yield strength of the chip material at room conditions, ε denotes the The equivalent plastic strain which is normalized with a reference strain rate denoted $\dot{\varepsilon}$ , $T_o$ is the ambient temperature, and the temperature at the melting point of the work material is denoted by $T_m$, which are both treated as constants in the current model. The effects of strain hardening of the material, thermal softening of the material and strain rate sensitivity are modelled by the parameters *n*, *m* and *C* respectively. Also, T represents machining temperature. The Johnson-Cook model is a duly validated equation and also it is a numerically strong material model which is extensively used in modelling and simulation studies.

Machining temperature is determined from Kronenbergs model as given below

$$T = \frac{C_o k_s V^{0.44} A_c^{0.22}}{W^{0.44} h^{0.56}}$$

Then remaining unknown terms equivalent plastic strain rate ε which is normalized with a reference strain rate $\dot{\varepsilon}$ are determined by using following equations respectively
Equivalent plastic strain

$$\varepsilon = \frac{\cot \emptyset + \tan(\emptyset-\alpha)}{\cos \varepsilon_f}$$

Equivalent plastic strain rate

$$\dot{\varepsilon} = \frac{2.59 \cdot V\varepsilon \sin \emptyset}{Depth\ of\ cut}$$

After finding the unknown terms we substitute these terms in Johnson cook equation to find out flow stress value

**Modeling of global forces on an end milling cutter**

Milling process could be treated as cutting with a series of cutting tools with single point cutting edges. Here the end mill tool cutting part is divided into number of slices which are aligned along axis of the tool (z direction). The forces due to cutting accomplished by each individual flute of each elementary cutter (or cutter slice) are determined using the oblique cutting model presented above. The total force on the entire milling cutter could be obtained by adding all the force vectors from all the flutes on all the slices. .

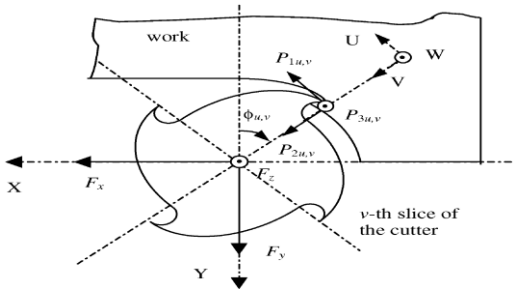


**Figure 4. Coordinate system for the vth slice** "[6]"

Milling is a discontinuous cutting process that is characterized by each tooth engaging or entering the work piece (i.e. starting cutting) at an angle $\emptyset_e$, known ar entering angle and disengaging or leaving the material at an angle $\emptyset_l$, known as leaving angle. In case of the up-milling $\emptyset_e$ = 0, since the width of cut in y direction will be dr, then $\emptyset_l$= arccos ((D − 2dr)/D). And in down-milling, $\emptyset_e$= arccos ((D − 2dr)/D), and $\emptyset_l$ =$\pi$. In slot milling, $\emptyset_e$= 0, and $\emptyset_l$ =$\pi$.
The net global cutting forces on the helical end milling cutter are shown in figure 3.4 and are represented below as

$$F_x(t) = \sum_{v=1}^{r} \sum_{u=1}^{Nt} (P_{1uv} \cos \emptyset_{uv} + P_{2uv} \sin \emptyset_{uv})$$

$$F_y(t) = \sum_{v=1}^{r} \sum_{u=1}^{Nt} (-P_{1uv} \sin \emptyset_{uv} + P_{2uv} \cos \emptyset_{uv})$$

$$F_x(t) = \sum_{v=1}^{r} \sum_{u=1}^{Nt} P_{3uv}$$

**Model Validation and Results**

For verifying this cutting force model presented in chapter 3, the experimental results from a series of tests performed using end milling cutters have been taken from H. Z. Li et.al "[6]". The tool used in these experiments was a plain shank short end milling with a diameter of 20 mm made of Sutton Co.8 high speed steel. The tools had four flutes with a helix angle of 30◦. Here the end milling tests were conducted at a spindle speed 600 rpm and the feed rate of 240 mm/min. The feed rate corresponds to 0.1 mm feed/tooth/revolution. The axial depth of cut is in the range between 5-12mm. The model presented in the previous chapter is used to simulate the experiments of H. Z. Li et.al[6] and a good agreement is obtained between their measurements and the current simulations. In what follows, several cases are presented where the predictions of the present model are plotted along with the measured cutting.

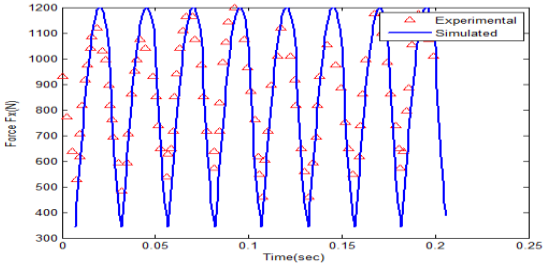


**Figure 5(a). Comparison for experimental and simulation cutting forces in X-direction for upmilling with axial depth of cut 8mm and speed 600rpm**

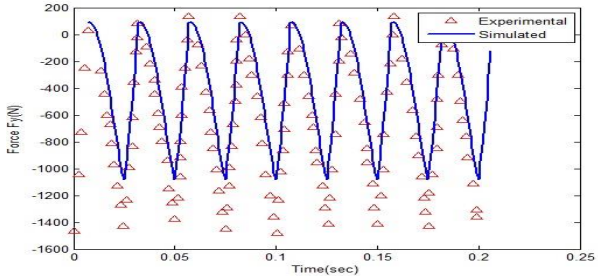


**Figure 5(b) Comparison for experimental and simulation cutting forces in Y-direction for upmilling with axial depth of cut 8mm and speed 600rpm.**

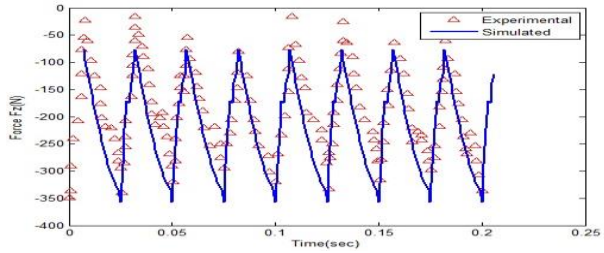


**Figure 5(c). Comparison for experimental and simulation cutting forces in Z-direction for upmilling with axial depth of cut 8mm and speed 600rpm**

**Figures 5(a), 5(b), 5(c). Comparison for experimental and simulation cutting forces for upmilling with axial depth of cut 8 mm**

Figures 5(a), 5(b), 5(c) shows the comparison between the predicted and measured cutting forces in x-, y-, and z-directions for upmilling with an axial depth of cut of 8 mm. Here it can be seen that the experimental and simulation wave forms agree within a reasonable accuracy and slight differences between these results could be due to cutter run out which is seen from the repeated tooth passing patterns from the experimental cutting forces.

Below figures 6(a), 6(b), 6(c) shows the comparison between the predicted and measured cutting forces in x-, y-, and z-directions for a different case where the axial depth of cut is 12 mm. Once again, there is a good agreement between the measured forces and the predictions made by the model.

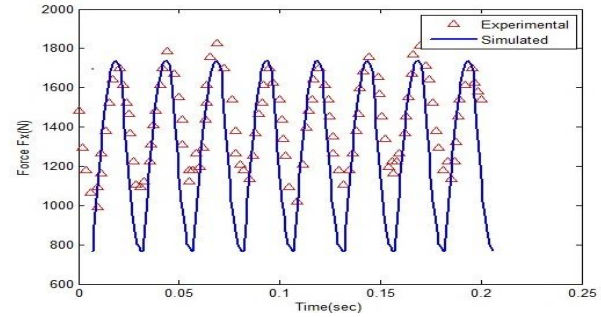


**Figure 6(a). Comparison between the predicted and measured cutting forces in X-direction for a different case where the axial depth of cut is 12 mm**

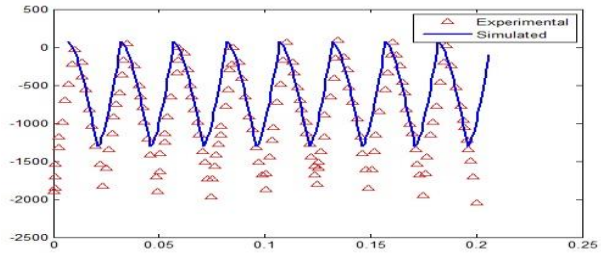


**Figure 6(b) . Comparison between the predicted and measured cutting forces in Y-direction for a different case where the axial depth of cut is 12 mm**

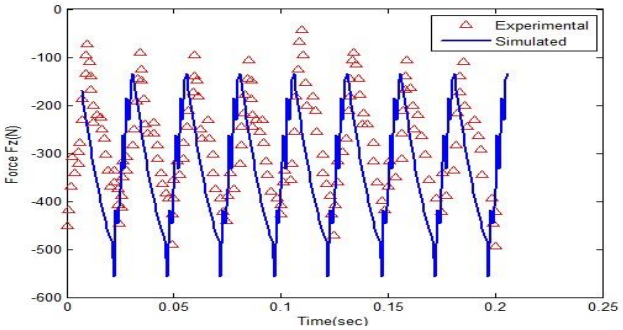


**Figure 6(c). Comparison between the predicted and measured cutting forces in Z-direction for a different case where the axial depth of cut is 12 mm**

**Figures 6(a), 6(b), 6(c) .Comparison for experimental and simulation cutting forces for up milling having axial depth of cut 12mm**

Tabke 4.1 presents a more direct numerical comparison between the average values of the measured cutting forces and those from the simulations made in the present study for three different cutting conditions. It can be seen from the table that or the majority of the cases the difference between the predictions and measurements is less than about 15%. The one exception is the y- direction force for the case where the axial depth of cut is 8 mm where the difference is about 37%. As already mentioned this difference is thought to be caused by tool run out which may be present in the experiments but is neglected in the modeling.

The model is also verified against a second set of experimental results which are taken from Chung-Liang Tsuai et al [18]. In their study cutting force was measured for a single cutting edge 16 mm radius end milling cutter performing peripheral milling with depth of cut is 1 mm, feed 1.33mm on 1045 steel with spindle speed of 1500 rpm . Table 4.2 shows the comparison between the measured average cutting force values reported by Chung-Liang Tsuai et al "[8]" and the average forces predicted using the current model. As can be seen from the table an excellent agreement was obtained between experiments and current model with the differences being less than about 5% which is within acceptable uncertainty levels.

Below figures 7(a), 7(b), 7(c) shows the comparison between the predicted and measure cutting forces in 3 directions during two complete revolutions of the tool. The forces are plotted against the tool rotation angle. It can be seen from the figure that the model predicts the measured cutting forces very closely. These two direct comparisons of model results with experiments are deemed to be adequate validation of the model presented in this study.

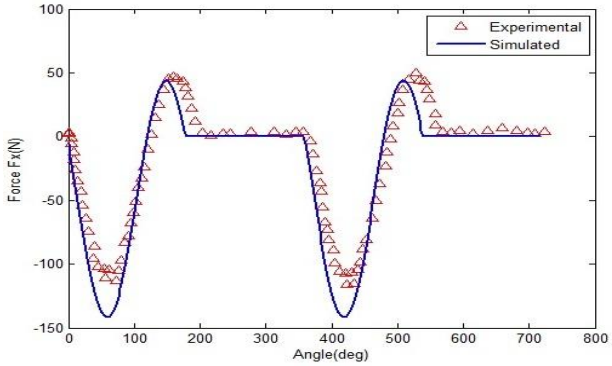


**Figure 7(a). Experimental and simulation of cutting force in X-direction of a single cutting edge end milling cutter in peripheral milling with depth of cut is 1 mm and speed 1500 rpm**

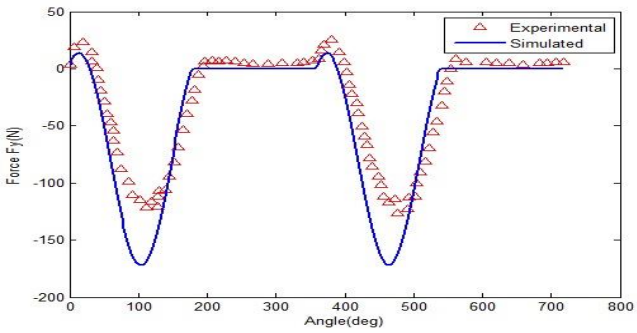


**Figure 7(b). Experimental and simulation of cutting force in Y-direction of a single cutting edge end milling cutter in peripheral milling with depth of cut is 1 mm and speed 1500 rpm**

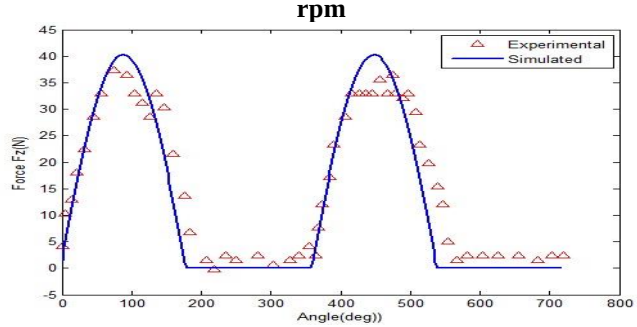


**Figure 7(c) . Experimental and simulation of cutting forces in Z-direction of a single cutting edge end milling cutter in peripheral milling with depth of cut is 1 mm and speed 1500 rpm**

**Figures 7(a), 7(b), 7(c). Experimental and simulation of cutting forces of a single cutting edge end milling cutter in peripheral milling with depth of cut is 1 mm.**

### 4.1. Parametric Study

A parametric study is conducted using the validated model to assess the effect of various cutting parameters on the generated cutting forces. The variables studied include

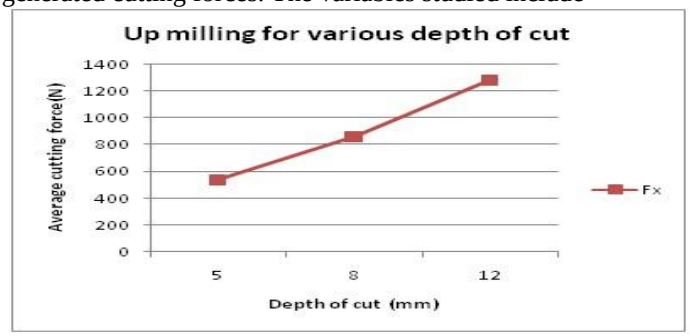


**Figure 8(a). Comparison between simulated cutting forces in X- direction with depth of cut as 5,8, 12mm and speed is 600 rpm**

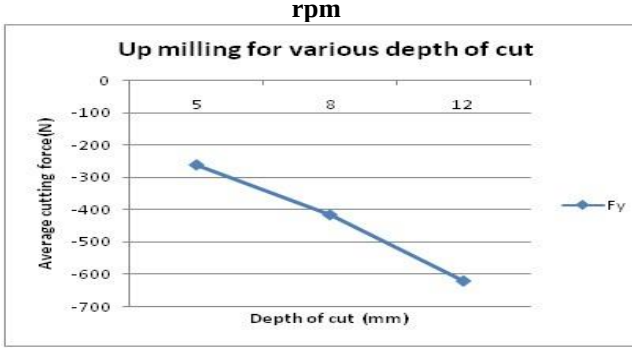


**Figure 8(b). Comparison between simulated cutting forces in Y- direction with depth of cut as 5,8, 12mm and speed is 600 rpm**

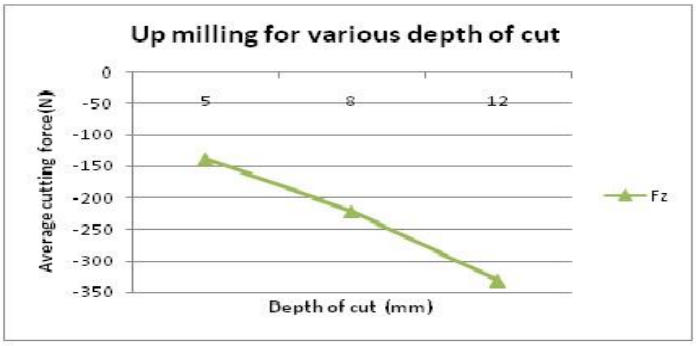


**Figure 8(c). Comparison between simulated cutting forces in Z- direction with depth of cut as 5,8, 12mm and speed is 600 rpm**

From this figures fig 8(a), fig 8(b), fig 8(c) the average simulated forces in x-direction increase linearly with increase in depth of cut and decrease linearly in y, z directions with increase in depth of cut

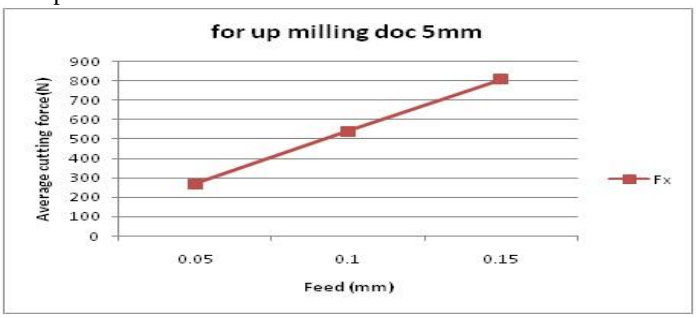


**Figure 9(a).Comparison between simulated cutting forces in X- direction with feed as 0.05, 0.1, 0.15mm for depth of cut 5mm and speed is 600 rpm**

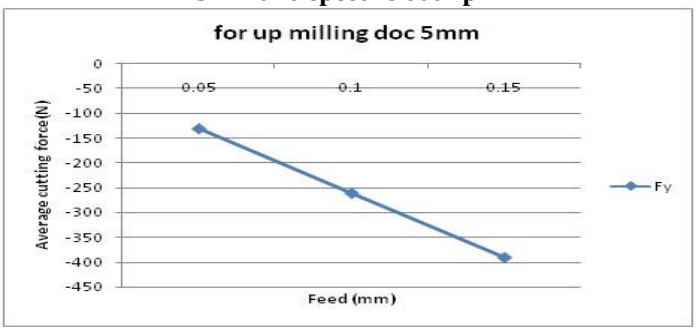


**Figure 9(b).Comparison between simulated cutting forces in Y- direction with feed as 0.05, 0.1, 0.15mm for depth of cut 5mm and speed is 600 rpm.**

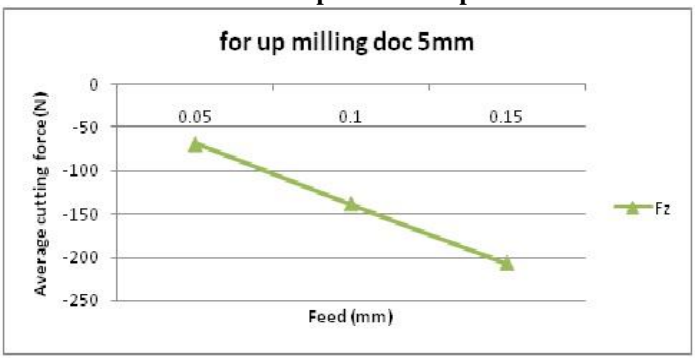


**Figure 9(c).Comparison between simulated cutting forces in Z- direction with feed as 0.05, 0.1, 0.15mm for depth of cut 5mm and speed is 600 rpm**

From this figures fig.9(a), fig.9(b), fig.9(c) the average simulated forces in x-direction increase linearly with in feed and decrease linearly in y, z directions with increase in feed

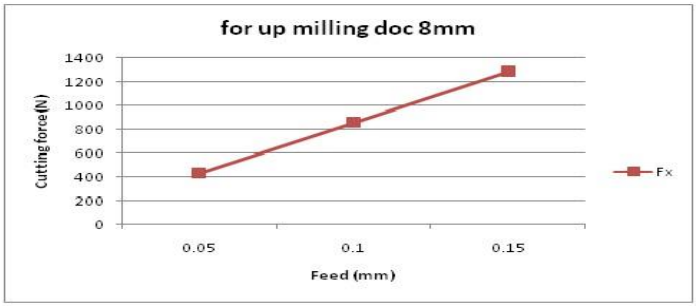


**Figure 10(a). Comparison between simulated cutting forces in X-directions with feed as 0.05,0.1, 0.15mm for depth of cut 8mm and speed is 600 rpm**

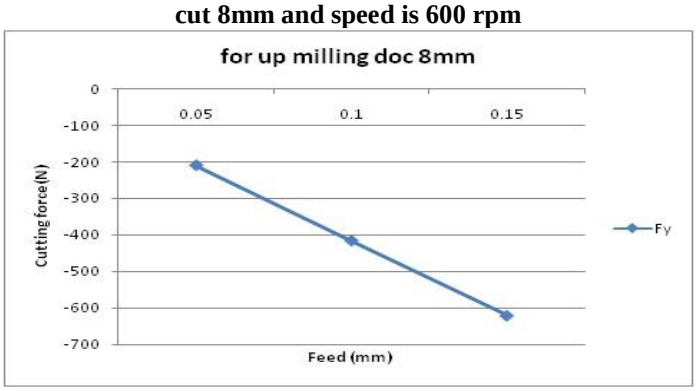


**Figure 10(b). Comparison between simulated cutting forces in Y-direction with feed as 0.05,0.1, 0.15mm for depth of cut 8mm and speed is 600 rpm**

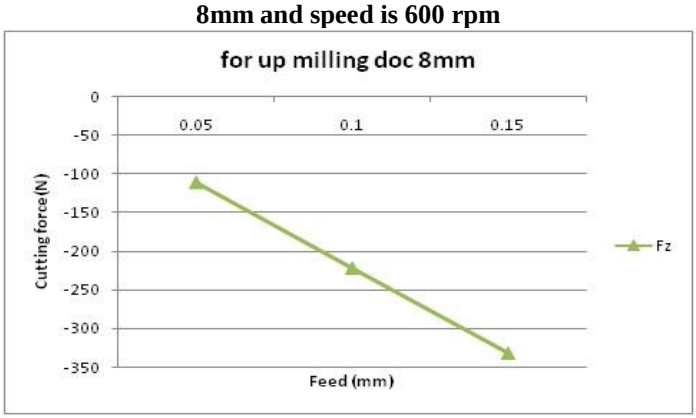


**Figure 10(c). Comparison between simulated cutting forces in Z-direction with feed as 0.05,0.1, 0.15mm for depth of cut 8mm and speed is 600 rpm**

**From this figures fig.10(a), fig.10(b), fig.10(c) the average simulated forces in x-direction increase linearly with increase in feed and decrease linearly in y, z directions with increase in feed**

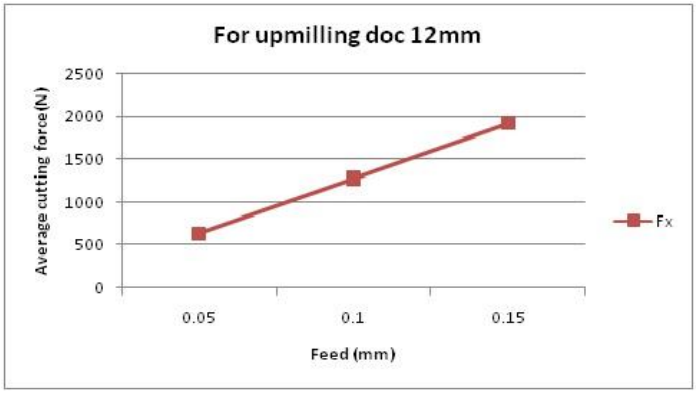


**Figure 11(a). Comparison between simulated cutting forces in X-directions with feed as 0.05,0.1, 0.15mm for depth of cut 12mm and speed is 600 rpm.**

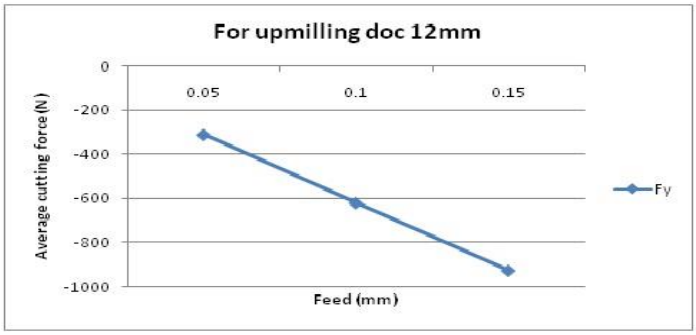


**Figure 11(b). Comparison between simulated cutting forces in Y-directions with feed as 0.05,0.1, 0.15mm for depth of cut 12mm and speed is 600 rpm**

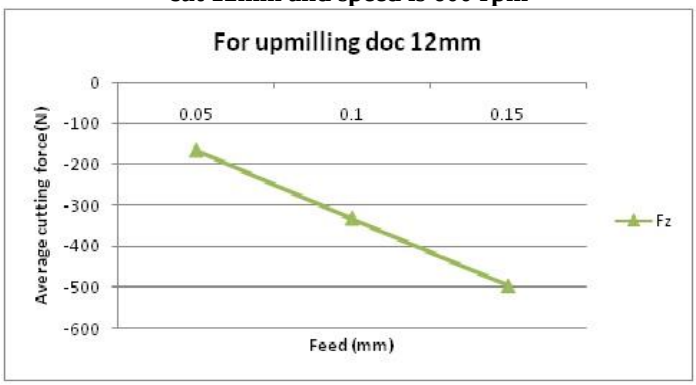


**Figure 11(c). Comparison between simulated cutting forces in X-directions with feed as 0.05,0.1, 0.15mm for depth of cut 12mm and speed is 600 rpm**

From this figures fig.11(a), fig.11(b), fig.11(c) the average simulated forces in x-direction increase linearly with increase in feed and decrease linearly in y, z directions with increase in feed

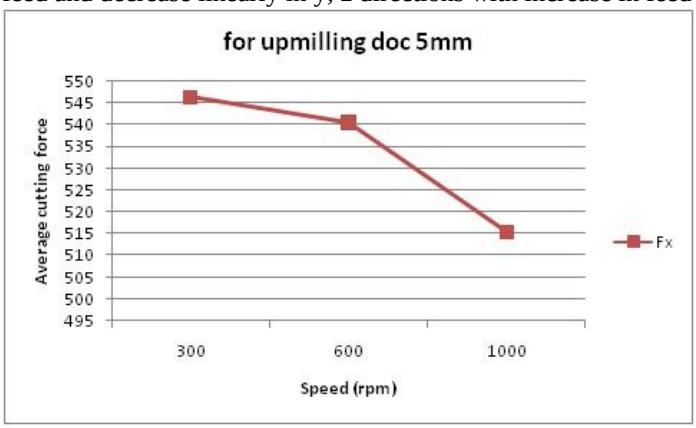


**Figure 12(a).Comparison between simulated cutting forces in X-direction with speed as 300, 600, 1000 rpm for depth of cut 5mm and feed is 0.1mm**

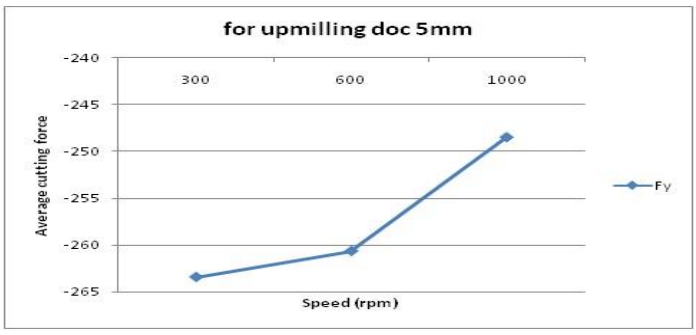


**Figure 12(b).Comparison between simulated cutting forces in Y-direction with speed as 300, 600, 1000 rpm for depth of cut 5mm and feed is 0.1mm**

**Table 1. Comparison between mean values of experimental and simulated cutting forces**

| Cutting Condition | Force direction | Averaged measured force(N) | Average simulated force(N) | Absolute Percentage |
|---|---|---|---|---|
| Up milling Doc =5mm | Fx | 558.587 | 540.5112 | 3.28 |
| | Fy | -375.353 | -260.6596 | 30.556 |
| | Fz | -118.459 | -138.7001 | 17.08 |
| Up milling Doc =8mm | FX | 893.466 | 858.9165 | 3.86 |
| | Fy | -664.094 | -414.9465 | 37.51 |
| | FZ | -191.965 | -221.7971 | 15.54 |
| Up milling Doc =12mm | Fx | 1364.740 | 1281.0 | 6.13 |
| | Fy | -900.181 | -619.7910 | 31.148 |
| | Fz | -285.022 | -331.5987 | 16.34 |

**Table 2. Comparison between mean values of experimental and simulated cutting forces**

| Cutting Condition | Force direction | Averaged measured force(N) | Average simulated force(N) | Absolute Percentage |
|---|---|---|---|---|
| peripheral milling Doc =1mm | Fx | -26.1971 | -24.4221 | 6.77 |
| | Fy | -38.8827 | -39.5433 | 1.69 |
| | Fz | 17.2208 | 12.8253 | 4.39 |

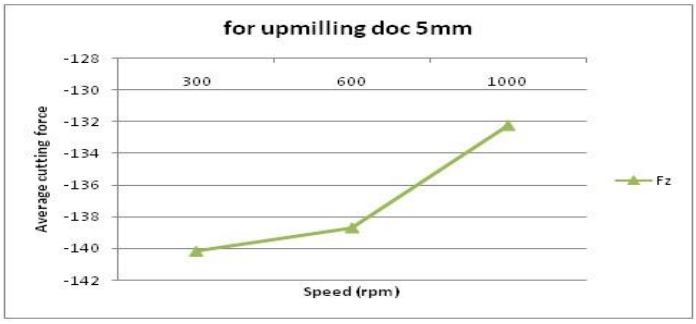


**Figure 12(c). Comparison between simulated cutting forces in Z-direction with speed as 300, 600, 1000 rpm for depth of cut 5mm and feed is 0.1mm**

From this figures fig.12(a), fig.12(b), fig.12(c) the average simulated forces in x-direction decrease with increase in speed and increase in y, z directions with increase in speed

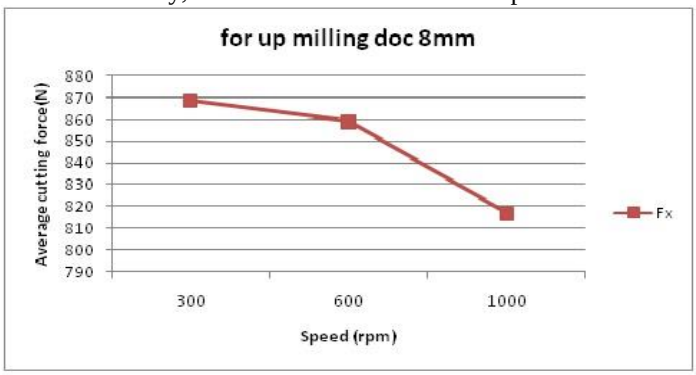


**Figure 13(a).Comparison between simulated cutting forces in X-direction with speed as 300, 600, 1000 rpm for depth of cut 8mm and feed is 0.1mm**

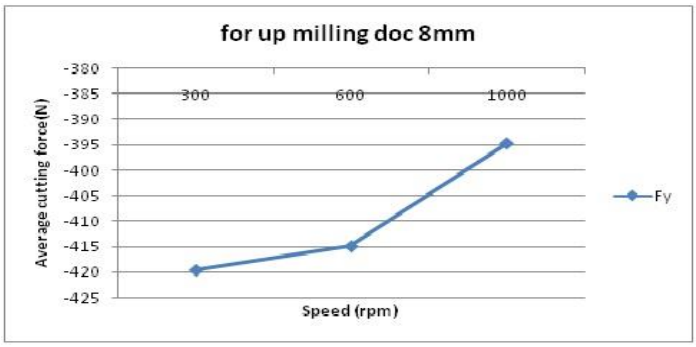


**Figure 13(b). Comparison between simulated cutting forces in Y-direction with speed as 300, 600, 1000 rpm for depth of cut 8mm and feed is 0.1mm**

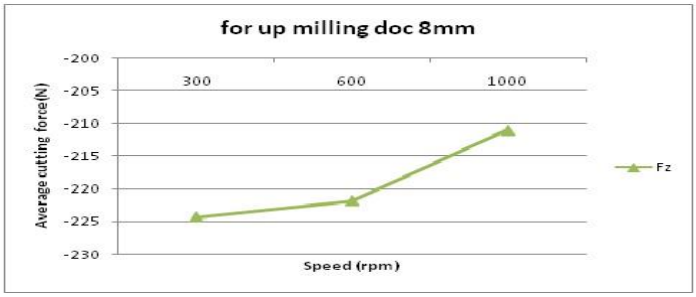


**Figure 13(c). Comparison between simulated cutting forces in Z-direction with speed as 300, 600, 1000 rpm for depth of cut 8mm and feed is 0.1mm**

From this figures fig.13(a), fig.13(b), fig.13(c) the average simulated forces in x-direction decrease with increase in speed and increase in y, z directions with increase in speed

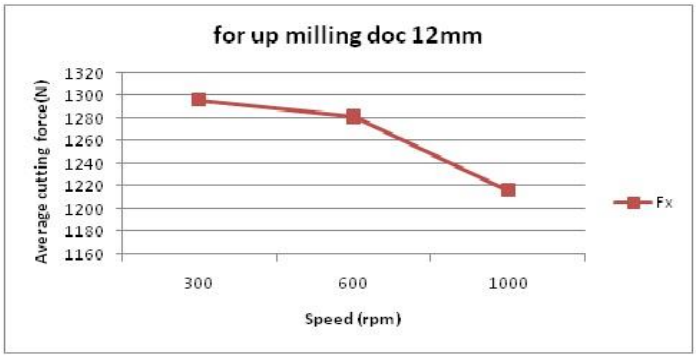


**Figure 14(a). Comparison between simulated cutting forces in X-direction with speed as 300, 600, 1000 rpm for depth of cut 12mm and feed is 0.1mm**

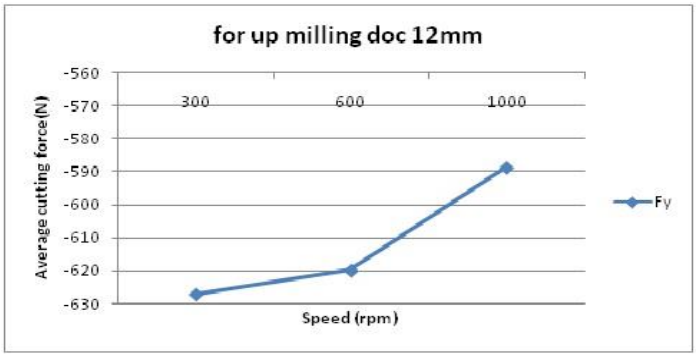


**Figure 14(b). Comparison between simulated cutting forces in Y-direction with speed as 300, 600, 1000 rpm for depth of cut 12mm and feed is 0.1mm**

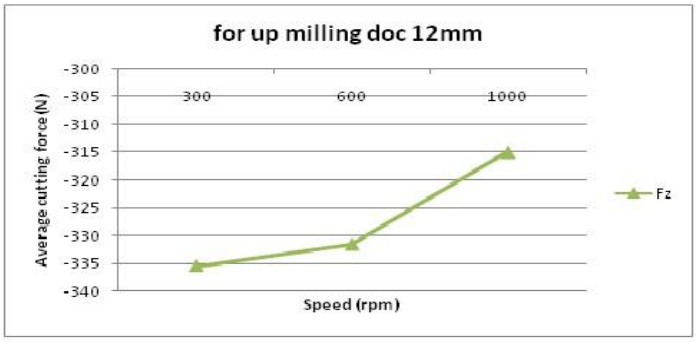


**Figure 14(c). Comparison between simulated cutting forces in Z-direction with speed as 300, 600, 1000 rpm for depth of cut 12mm and feed is 0.1mm**

From this figures fig.14(a), fig.14(b), fig.14(c) the average simulated forces in x-direction decrease with increase in speed and increase in y, z directions with increase in speed

**Conclusion**

In this project a predictive cutting force model has been developed for the prediction of cutting forces in helical end milling. In this the influencing factors on the cutting forces of a helical end milling are depth of cut, feed, speed and instaneous rotation angles and also effect on the tool tip. The predictive model is based on the oxleys predictive machining theory in which machining parameters can be obtained from the input data of work piece material properties, tool geometry and their cutting conditions. The flow stress of the work piece is predicted from the Johnson cook constant model. In this predictive cutting force model the end mill cutter is divided into number of slices which accounts along its axis to the helix angle. This model is used in end milling cutter of up milling and peripheral milling. The total forces which are acting on the cutter are referred as sum of forces on each tooth segment of the slice. The cutting action of the tooth is modeled as oblique cutting. The cutting actions of slices on each tooth in which first cutting slice and the rest of cutting slices are also modeled as oblique cutting without end cutting edge effect and tool nose radius effect. The simulated values obtained from the cutting force model are found match very well with experimental values..

**References**

[1]. C.A.C. Antonio, J.P. Davim titled with "Optimal cutting conditions in turning Of particulate metal matrix composites based on experimental and a Genetic search model", Composites: Part A 33 (2002) 213–219.

[2]. D.B. Miracle titled with "Metal *matrix composites* – From science to technological significance" Composites Science and Technology 65 (2005) pp. 2526–2540.

[3]. N. Narutaki, "Machining of MMCs", VDI BERICHTE NR 1276 (1996) 359–370.

[4] Karakas, M. S., Acir Adem., Ubeyli Mustafa and Ogel Bilgehan., "Effect of cutting speed on tool performance in milling of B4CP reinforcement aluminium metal matrix composite", Journal of materials processing technology, 178 (2006) pp. 241-246.

[5]. Oxley PLB. Mechanics of Machining. Chichester: Ellie Horwood Limited, 1989.

[6]. H.Z. Li titled with "Modelling of cutting forces in helical end milling using a predictive machining theory". International Journal of Mechanical Sciences February 2001.

[7]. Fontaine M., A., Devillez " Predictive force model for ball-end milling and experimental validation with a wavelike from machining test" International journal of machine tool and manufacture, 46 (2002) pp.367-380

[8]. Chung-Liang Tsai titled with "Analysis and prediction of cutting forces in end milling by means of a geometrical model". International Journal of Advance Manufacture technology March 2006.

[9]. Budak E., Altintas Y., and Armarego E.A.; "Prediction of milling force coefficients from orthogonal cutting data" *ASME Vol.* 118(1996) pp. 216-224.